Minimizing Bit Error Probability for Chromatic and Polarization-Mode Dispersion by Optimized Receiver Filters for Various Optical Modulation Formats

Torsten Freckmann and Joachim Speidel, Institut für Nachrichtenübertragung, Universität Stuttgart,
Pfaffenwaldring 47, D-70569 Stuttgart, Email: torsten.freckmann@inue.uni-stuttgart.de

Abstract

The scope of this paper is two-fold: First, we show how to extend the Karhunen-Loève series expansion method to calculate the bit error probability in optical transmission systems with direct detection. The extension allows us to take account of not only chromatic dispersion but also polarization-mode dispersion. Second, we investigate the impact of receiver filter bandwidths on the chromatic and polarization-mode dispersion tolerance of various modulation formats. We show that the chromatic dispersion tolerance can be significantly increased by narrow optical filtering for all investigated modulation formats especially if return-to-zero impulse shaping is applied.

1 Introduction

The limiting effects besides fiber nonlinearities in optical communications systems of high bitrates are chromatic dispersion (CD) and polarization-mode dispersion (PMD). Therefore, it becomes more and more important for future optical data transmission to improve the tolerance towards these fiber impairments. In recent times a lot of research was dedicated to this problem. On the one hand, multilevel optical modulation formats have been investigated [1]–[4]. Since more than one bit per symbol is allocated the transmission rate on the fiber is lower than the actual bitrate. This leads to a higher tolerance towards both CD and PMD – however to the cost of lower receiver sensitivity. On the other hand, it has been shown, that optical and electronic equalization can significantly improve the dispersion tolerance for optical binary amplitude-shift keying (ASK) [5], [6]. Applied to more advanced modulation formats like differential binary phase-shift keying (DBPSK) or differential quadrature phase-shift keying (DQPSK) electronic equalization seems to be less effective [7], [8].

In this paper we show in the first part how to extend a method for the analytical evaluation of the bit error probability (BEP) for optical communication systems with direct detection to the effect of PMD. The method is based on a Karhunen-Loève series expansion (KLSE) and will therefore be called the KLSE method in the following. Even though originally presented for ASK with arbitrary pulse shape, optical and electrical filtering, and CD in [9], it has been shown e.g. in [10], [11] that it can also be applied to DPSK systems. Here we will show how the KLSE method is further extended to take into account the effect of PMD.

In the second part we investigate the impact of receiver (RX) filter 3 dB bandwidths (BW) on the tolerance of ASK, DBPSK, and DQPSK towards CD and first-order PMD. We show that the optimal BWs depend on the amount of CD and PMD. We further show that the tolerable amount of CD until reaching an optical signal-to-noise ratio (OSNR) penalty of 3 dB can be increased by narrow optical filtering by about 30% for RZ-ASK and about 60% for RZ-DBPSK. For NRZ-ASK, NRZ-DBPSK, and DQPSK (both NRZ and RZ) a significant improvement can (if at all) only be observed for even higher penalties of more than 3 dB. The influence of RX filter BWs on the PMD tolerance is rather small.

The paper is organized as follows. In section 2 we present the basic system model investigated in this paper. The extension of the KLSE method to take account of PMD is described in section 3. An investigation of the influence of RX filter BWs on the CD and PMD tolerance will be presented in section 4, where we will also give optimal optical and electrical BWs as a function of the amount of CD or PMD. A summary in section 5 concludes the paper.

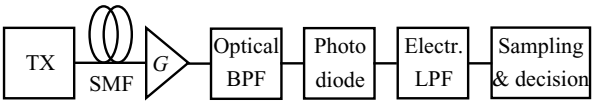

Fig. 1. System model for fiber optic ASK transmission

2 System Model

Fig. 1 shows the block diagram of a fiber communication system using ASK. The transmitter (TX) consists of a pseudo random bit sequence generator and a continuous wave laser which is modulated externally by a Mach-Zehnder modulator (MZM), [11]. The electrical drive signal of the MZM is generated from the bit sequence by impulse shapers with raised-cosine (RC)

Freckmann, T.; Speidel, J.: "Minimizing Bit Error Probability for Chromatic and Polarization-Mode Dispersion by Optimized Receiver Filters for Various Modulation Formats, ITG-Fachtagung Photonische Netze, Leipzig, Germany, April 2006, p.p. 235-242.

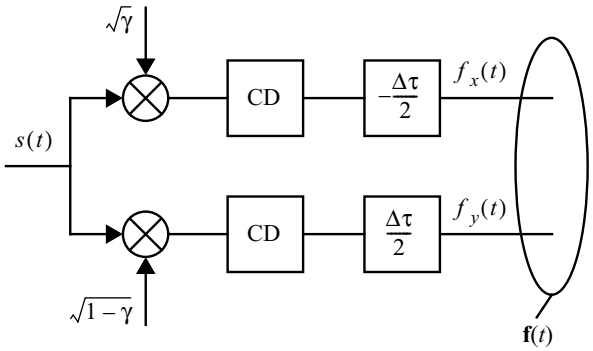

Fig. 2. Equivalent low-pass model of SSMF with CD and PMD

impulse responses

$$h(t)=\begin{cases}1 & ,|t|\le\frac{T}{2}(1-\alpha)\\ \cos^2\left[\frac{\pi}{4}\frac{2|t|-T(1-\alpha)}{\alpha T}\right] & ,\frac{T}{2}(1-\alpha)<|t|<\frac{T}{2}(1+\alpha)\\ 0 & ,|t|\ge\frac{T}{2}(1+\alpha)\end{cases}. \tag{1}$$

$T=1/R_s$ is the symbol duration and α is the roll-off factor, which is set to 0.5 throughout this paper. R_s is the symbol rate. It is worth to mention that the following BEP calculation is not restricted to the assumption of RC impulse shaping, which is considered here as an example only. Return-to-zero (RZ) impulse shaping with 50% duty cycle is achieved by modulating the amplitude of the non-return-to-zero (NRZ) signal in a subsequent MZM with a sinusoidal pulse.

The single mode fiber (SMF) in Fig. 1 includes CD and first-order PMD. We assume that the fiber is lossless. In this case we can use the principal states model to characterize first-order PMD and describe the SMF as a one-input two-output device, with each output corresponding to an output principal state of polarization (PSP) as depicted in **Fig. 2**. The transfer function of the SMF may then be written in vector notation as [10]

$$\mathbf{H}_f(f)=\begin{pmatrix}\sqrt{\gamma}\exp\left[j2\pi f\left(-\frac{\Delta\tau}{2}\right)+j\frac{\lambda^2 DL}{4\pi c}(2\pi f)^2\right]\\ \sqrt{1-\gamma}\exp\left[j2\pi f\left(\frac{\Delta\tau}{2}\right)+j\frac{\lambda^2 DL}{4\pi c}(2\pi f)^2\right]\end{pmatrix}, \tag{2}$$

where the first line applies to the *x*-polarization and the second line to the *y*-polarization, respectively. In (2) γ is the power splitting ratio, indicating how the input light power is projected on the two PSPs and $\Delta\tau$ represents the differential group delay (DGD). D is the fiber CD parameter, which is assumed to have a typical value of $17\,\mathrm{ps/(nm\cdot km)}$, L is the fiber length, c is the velocity of light, and $\lambda=1550\,\mathrm{nm}$ is the operating wavelength.

The RX is the cascade of a 2nd order optical Gaussian band-pass and a 3rd order electrical Bessel low-pass filter with a photo diode (PD) in between followed by a sampler and a binary decision device.

For DBPSK the TX is very similar to the one for ASK. The only difference is that the bit sequence is differentially encoded and the MZM is biased in such a way that the TX output signal $s(t)$ can take on two different phase angles $\varphi(t_0+kT)=\varphi_k\in\{0,\pi\}$ at sampling instants $t=t_0+kT$. The RX uses a delay & add interferometer filter (DAF) followed by a balanced detector instead of the single PD [12]. For DQPSK we use two parallel MZMs in the TX leading to a TX output signal $s(t)$ that can then take on four different phase angles $\varphi_k\in\{\frac{\pi}{4},\frac{3\pi}{4},\frac{5\pi}{4},\frac{7\pi}{4}\}$. The RX uses two DAFs to recover the information symbols [1].

3 Analytical Calculation of Bit Error Probability

We now briefly sketch how to extend the KLSE method used to calculate the BEP for ASK in order to take PMD into account. In recent times the KLSE method has been reported in various closely related variants for fibers with CD. We adopt a variant that is mainly based on [9], however, with some changes which we have earlier presented in [11]. We shall mention that the following calculations are not restricted to first-order PMD but may also be conducted in the same way for higher-order PMD. We have restricted ourselves to first-order effects since this is a reasonable approximation according to [13]. Moreover, it allows a simple and computationally efficient channel model.

Before presenting more details of the calculation we shall have a closer look at the opto-electronic conversion process at the RX. The PD is inherently polarization insensitive since it detects the instantaneous incident optical power. The PD may therefore be modelled as a quadratic detector

$$|\mathbf{v}(t)|^2=\left|\begin{pmatrix}v_x(t)\\ v_y(t)\end{pmatrix}\right|^2=|v_x(t)|^2+|v_y(t)|^2, \tag{3}$$

followed by a low-pass filter. In (3) $\mathbf{v}(t)$ is the incident electrical field with $v_x(t)$ and $v_y(t)$ denoting the field in *x*- and *y*-polarization, respectively. According to the right hand side of (3) the photo current is given by the sum of the optical power associated with the two PSPs. This motivates the equivalent low-pass model of the ASK RX in **Fig. 3**, where both PSPs are processed seperately.

Now, with the same assumptions as in [11], namely, that the bit sequence at the TX and hence all deterministic signals are periodic with a period of K symbol intervals and that amplified spontaneous emission from the optical amplifier in Fig. 1 is the dominant noise source we can briefly sketch the BEP calculation. The RX noise can be modeled by two independent identically distributed (i.i.d.) complex additive white Gaussian noise sources $w_x(t)$ and $w_y(t)$ with zero mean in front of the optical RX filter as depicted in Fig. 3. Following the calculations in [11] we can write the sample g_k at the RX in Fig. 3 as a quadratic form:

$$g_k=\mathbf{v}_{x,k}^H\mathbf{H}_{\mathrm{el}}\mathbf{v}_{x,k}+\mathbf{v}_{y,k}^H\mathbf{H}_{\mathrm{el}}\mathbf{v}_{y,k}, \tag{4}$$

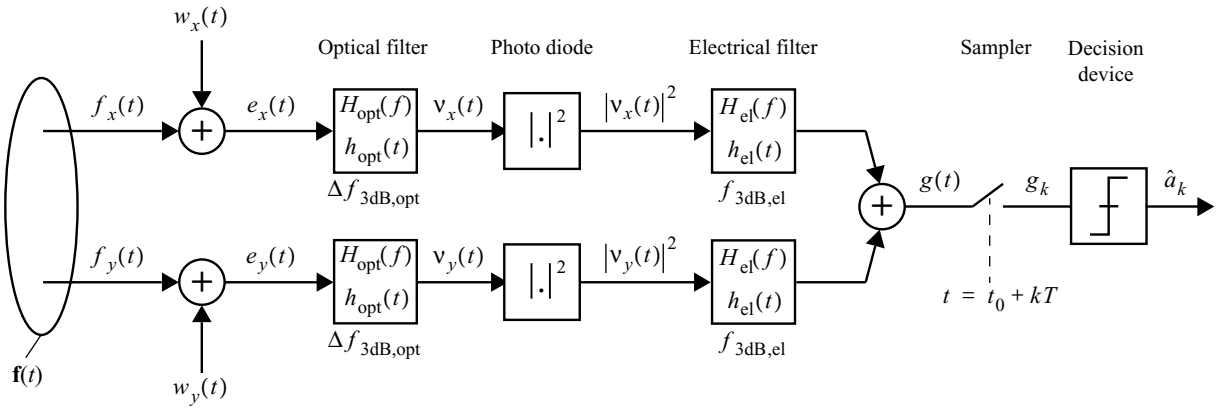

Fig. 3. Equivalent low-pass model of the ASK receiver for PMD.

where $\mathbf{v}_{x,k} = \mathbf{z}_{x,k} + \mathbf{n}_{x,k}$ and $\mathbf{v}_{y,k} = \mathbf{z}_{y,k} + \mathbf{n}_{y,k}$ are random vectors consisting of samples of $v_x(t) = z_x(t) + n_x(t)$ and $v_y(t) = z_y(t) + n_y(t)$ at time instants $t = t_0 + (kM - m)\Delta t$ $(m = 0, 1, \ldots, N-1)$, respectively. M is the oversampling factor, $\Delta t = T/M$, and $N = M \cdot K$. The diagonal matrix $\mathbf{H}_{\text{el}}$ is the same for both RX branches and contains samples of the electrical filter impulse response $h_{\text{el}}(t)$ on the main diagonal.

If we form a new vector $\hat{\mathbf{v}}_k$ by simply stacking $\mathbf{v}_{x,k}$ and $\mathbf{v}_{y,k}$, we can rewrite (4) to obtain

$$g_k = \begin{pmatrix} \mathbf{v}_{x,k} \\ \mathbf{v}_{y,k} \end{pmatrix}^H \cdot \begin{pmatrix} \mathbf{H}_{\text{el}} & \mathbf{0} \\ \mathbf{0} & \mathbf{H}_{\text{el}} \end{pmatrix} \cdot \begin{pmatrix} \mathbf{v}_{x,k} \\ \mathbf{v}_{y,k} \end{pmatrix} = \hat{\mathbf{v}}_k^H \hat{\mathbf{H}}_{\text{el}} \hat{\mathbf{v}}_k, \quad (5)$$

where $\hat{\mathbf{v}}_k$ has length $2N$ and $\hat{\mathbf{H}}_{\text{el}}$ is a $2N \times 2N$ matrix. With the right hand side of (5) we have obtained a form of the decision variable g_k which directly corresponds to the one in [11]. As a consequence we can find the following equation for the moment generating function (MGF) of g_k:

$$M_{g_k}(p) = \prod_{n=1}^{2N} \frac{\mathrm{e}^{\frac{p\lambda_n |\eta_n|^2}{1-p\lambda_n}}}{1 - p\lambda_n}, \quad (6)$$

In (6) λ_n denote the eigenvalues of $\hat{\mathbf{C}} \cdot \hat{\mathbf{H}}_{\text{el}}$, where $\hat{\mathbf{C}}$ is the correlation matrix of $\hat{\mathbf{n}}_k = \left(\mathbf{n}_{x,k}, \mathbf{n}_{y,k}\right)^T$, which is given by

$$\hat{\mathbf{C}} = \mathrm{E}\left[\hat{\mathbf{n}}_k \cdot \hat{\mathbf{n}}_k^H\right] = \mathrm{E}\left[\begin{pmatrix} \mathbf{n}_{x,k} \\ \mathbf{n}_{y,k} \end{pmatrix} \cdot \begin{pmatrix} \mathbf{n}_{x,k} \\ \mathbf{n}_{y,k} \end{pmatrix}^H\right] = \begin{pmatrix} \mathbf{C}_{xx} & \mathbf{C}_{xy} \\ \mathbf{C}_{xy}^H & \mathbf{C}_{yy} \end{pmatrix}. \quad (7)$$

Since the noise sources $w_x(t)$ and $w_y(t)$ were assumed to be i.i.d. we can conclude that $\mathbf{C}_{xx} = \mathbf{C}_{yy} = \mathbf{C}$ and $\mathbf{C}_{xy} = \mathbf{0}$. As a consequence the eigenvalues λ_n occur with multilplicity two and it is sufficient to calculate the eigenvalues of $\mathbf{C} \cdot \mathbf{H}_{\text{el}}$ instead of those of $\hat{\mathbf{C}} \cdot \hat{\mathbf{H}}_{\text{el}}$, which is computationally much more efficient.

The η_n in (6) are the elements of the vector $\hat{\boldsymbol{\eta}}_k = \left(\boldsymbol{\eta}_{x,k}, \boldsymbol{\eta}_{y,k}\right)^T$ which results when applying a Karhunen-Loève coordinate transform to $\mathbf{z}_{x,k}$ and $\mathbf{z}_{y,k}$ as in [11]. Since the probability density function of the RX sample g_k is given by the inverse Laplace transform (LT) of $M_{g_k}(-p)$, the BEP may be obtained from an inverse Laplace integral, which after some calculations finally results into [14]

$$P_{e,k} = \pm \frac{1}{2\pi j} \int_{\sigma - j\infty}^{\sigma + j\infty} \frac{M_{g_k}(p)}{p} \mathrm{e}^{-pE_{\text{th}}} dp, \quad (8)$$

where we used the integration property of the LT. In (8) the positive sign applies if at the considered discrete time instant k a zero was transmitted and the negative sign applies if a one was transmitted. Moreover, E_{th} denotes the decision threshold, which is optimized to yield minimum BEP.

The contour integral in (8) can for reasonable accuracy be evaluated with the saddle point approximation leading to the closed form expression [9]

$$P_{e,k} = \pm \frac{\mathrm{e}^{\phi(\sigma_0)}}{\sqrt{2\pi\phi''(\sigma_0)}}. \quad (9)$$

Where $\phi(p) = \ln\left(M_{g_k}(p)\right) - \ln(p) - pE_{\text{th}}$ is the natural logarithm of the integrand of (8) and σ_0 denotes the saddle point of $\phi(p)$, which may be found as the root of the first derivative $\phi'(p)$ of $\phi(p)$.

The extension of the KLSE method to DBPSK and DQPSK transmission is presented e.g. in [14] and [10] and is straightforward. The main difference is that the incorporated vectors and matrices are two times as large if balanced detection is assumed and the DQPSK RX is regarded as two parallel DBPSK RX.

4 Optimization of Receiver Filter Bandwidths

With the analytical method described in the previous section we calculate the required OSNR to achieve a BEP of 10^{-9}. We investigate three different modulation formats, namely, ASK, DBPSK and DQPSK transmission. For all modulation formtas the same data rate of 40 Gb/s is assumed and various link configurations are examined. We show that the optical and the electrical RX filter 3 dB BWs (in the following just called optical BW and electrical BW, respectively) have a great

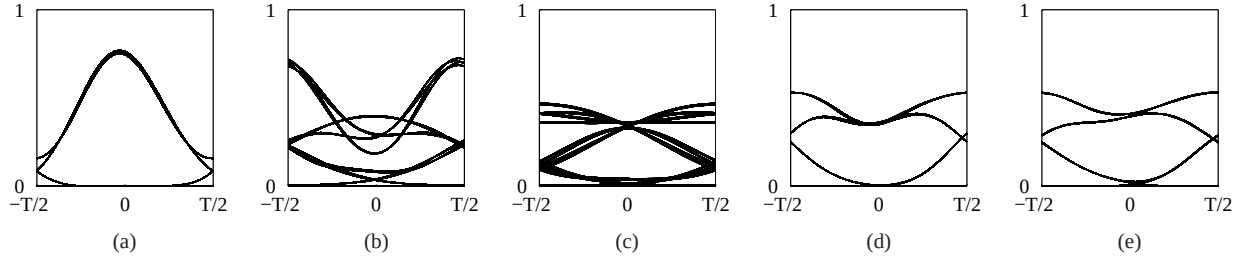

Fig. 4. Normalized eye diagrams at decision device for RZ-ASK: (a) back-to-back, (b) $R_d = 68$ ps/nm with back-to-back BWs, (c) $R_d = 68$ ps/nm with optimized BWs, (d) $\Delta\tau = 15$ ps with back-to-back BWs, and (e) $\Delta\tau = 15$ ps with optimized BWs

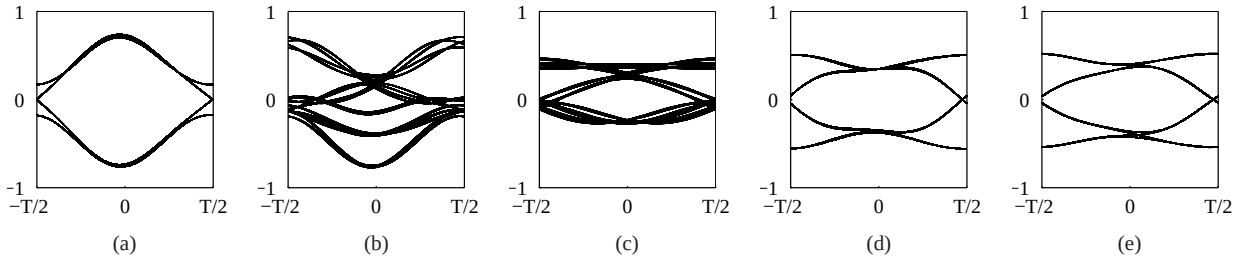

Fig. 5. Normalized eye diagrams at decision device for RZ-DBPSK: (a) back-to-back, (b) $R_d = 68$ ps/nm with back-to-back BWs, (c) $R_d = 68$ ps/nm with optimized BWs, (d) $\Delta\tau = 15$ ps with back-to-back BWs, and (e) $\Delta\tau = 15$ ps with optimized BWs

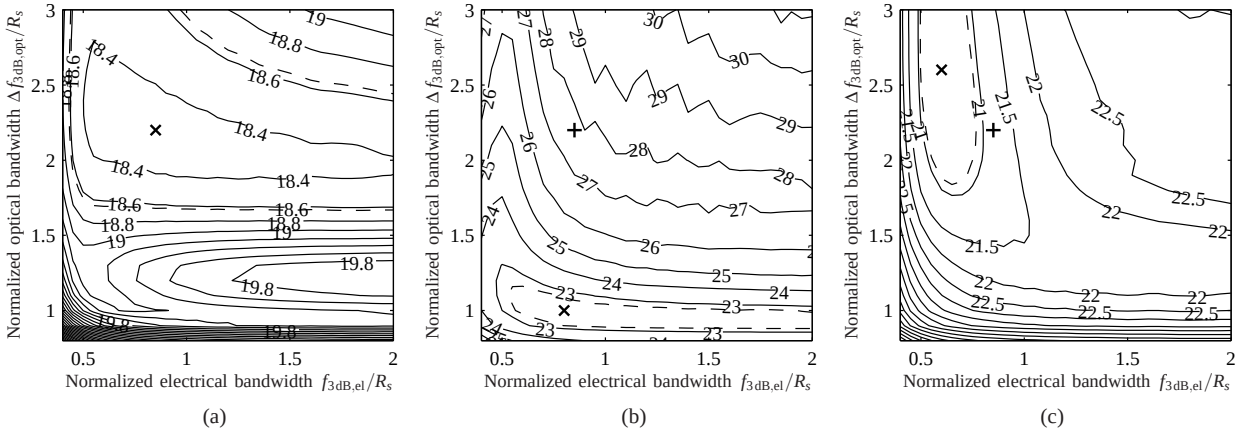

Fig. 6. Required OSNR for BEP $= 10^{-9}$ vs. optical and electrical receiver BWs for RZ-ASK: (a) back-to-back, (b) $R_d = 68$ ps/nm and $\Delta\tau = 0$ ps, and (c) $R_d = 0$ ps/nm and $\Delta\tau = 15$ ps

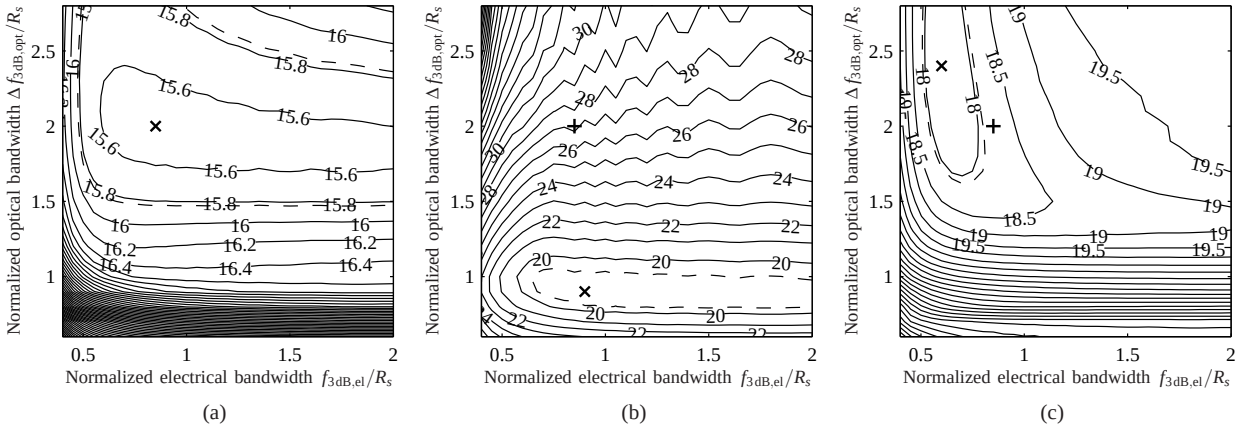

Fig. 7. Required OSNR for BEP $= 10^{-9}$ vs. optical and electrical receiver BWs for RZ-DBPSK: (a) back-to-back, (b) $R_d = 102$ ps/nm and $\Delta\tau = 0$ ps, and (c) $R_d = 0$ ps/nm and $\Delta\tau = 15$ ps

influence on the performance. In recent times a lot of work was elaborated to assess optimal RX filter BWs for various modulation formats (see e.g. [15]–[17]). However, these studies were limited to the case of a fully compensated fiber link, which is often — and therefore also in the following — called the back-to-back (b2b) case. We will show that CD and PMD tolerance[1] may be increased by optimizing the optical and the electrical BW with respect to CD and PMD.

A first hint on this fact can be observed from **Figs. 4** and **5** where we present normalized eye diagrams at the decision device for RZ-ASK in Fig. 4 and for RZ-DBPSK in Fig. 5. Subfigures (a) show b2b eye diagrams as a reference. In Figs. 4(b),(c) and 5(b),(c) PMD is absent and the residual dispersion equals $R_d = 68\,\text{ps/nm}$ for ASK and $R_d = 102\,\text{ps/nm}$ for DBPSK. Whereas in subfigures (b) the BWs are adjusted like in the b2b case, subfigures (c) show the eye diagrams for optimized BWs. Note that the scaling of the ordinate is different in Fig. 4 compared to Fig. 5. One can observe that optimizing the BWs with respect to the residual dispersion significantly increases the eye-opening and thus lowers the required OSNR to achieve a certain BEP, as it will be shown later. Moreover, it becomes appearent especially from Fig. 4(b) that when using b2b BWs the sampling instant at the receiver has to be optimized since the largest eye-opening is no longer at the middle of the symbol duration. If RX filter BWs are optimized as in Fig. 4(c) an optimization of the sampling instant is no longer required, since the largest eye-opening is now again observed at the middle of the symbol duration. We shall mention that we have optimized the sampling instant for all calculations of the required OSNR presented in this paper.

Eye diagrams for the case when CD is absent and the DGD equals $\Delta\tau = 15\,\text{ps}$ are presented in Figs. 4(d),(e) and 5(d),(e). Again subfigures (d) show the case of BWs adjusted like in the b2b case, whereas subfigures (e) were obtained with optimized BWs. It becomes obvious that an optimization of the BWs does not result in a significant improvement of the eye-opening and will therefore not have much impact on the required OSNR.

Fig. 6 and **Fig. 7** show contour plots of required OSNR for $\text{BEP} = 10^{-9}$ vs. electrical and optical BWs normalized to the symbol rate R_s for RZ-ASK and RZ-DBPSK, respectively. Subfigures (a) show the results for the b2b case, subfigures (b) for the case where PMD is absent and the residual dispersion equals $R_d = 68\,\text{ps/nm}$ for RZ-ASK and $R_d = 102\,\text{ps/nm}$ for RZ-DBPSK, and subfigures (c) for the case where CD is absent and the DGD equals $\Delta\tau = 15\,\text{ps}$. In each plot the BW pair which leads to the lowest required OSNR is marked with '$\times$'. Moreover in subfigures (b) and (c) the BW pair which is optimal for the b2b case marked with '$+$'. The dashed curves in Figs. 6 and 7 correspond to the 0.3 dB tolerance region around the optimum. Note that all plots are equally scaled but the value ranges may differ. As we could already expect from the eye diagrams in Figs. 4 and 5 it turns out that for the case where only CD is present (cf. Figs. 6(b) and 7(b)) the optimal BW pair and the BW pair for the b2b case differ considerably. If the BW would not be optimized dependent on the amount of CD we would observe an additional OSNR penalty of about 5 dB for RZ-ASK in Fig. 6(b) and even more than 7 dB for RZ-DBPSK in Fig. 7(b). For the case where only PMD is present, we can observe from Figs. 6(c) and 7(c) that the b2b BW pair is located very closely to the 0.3 dB tolerance region around the optimal BW pair. Thus, we observe only an almost negligible additional OSNR penalty of less than 0.5 dB.

Moreover, we can see in Figs. 6(b) and 7(b) that for the case where only CD is peresent the 0.3 dB tolerance region spans almost the whole considered electrical BW range from $0.4\ldots2\cdot R_s$, whereas it is rather narrow with respect to the optical BW $\Delta f_{3\text{dB,opt}}$. Opposed to that, for the case where only PMD is present (cf. Figs. 6(c) and 7(c)), the 0.3 dB tolerance region is rather narrow with respect to the electrical BW $f_{3\text{dB,el}}$, but reaches from about $1.7\cdot R_s$ beyond $3\cdot R_s$ for the optical BW.

We performed the same investigations for NRZ-ASK and NRZ-DBPSK. However, it turns out that the OSNR penalty may not be significantly improved by optimizing the BWs dpendent on the amount of CD or PMD for NRZ impulse shaping as will be shown later. Nevertheless, we have included NRZ transmission in **Table 1** and **Table 2**, which summarize the optimal BWs for the cases presented in Figs. 6 and 7 for ASK and DBPSK, respectively.

Table 1
Optimal optical and electrical receiver filter BWs for ASK

SMF	back-to-back		$R_d = 68\,\text{ps/nm}$		$\Delta\tau = 15\,\text{ps}$	
configuration	NRZ	RZ	NRZ	RZ	NRZ	RZ
$\Delta f_{3\text{dB,opt}}/R_s$	1.2	2.2	1.1	1.0	1.3	2.6
$f_{3\text{dB,el}}/R_s$	1.00	0.85	1.30	0.80	2.35	0.60

Table 2
Optimal optical and electrical receiver filter BWs for DBPSK

SMF	back-to-back		$R_d = 102\,\text{ps/nm}$		$\Delta\tau = 15\,\text{ps}$	
configuration	NRZ	RZ	NRZ	RZ	NRZ	RZ
$\Delta f_{3\text{dB,opt}}/R_s$	1.2	2.0	0.9	0.9	2.3	2.4
$f_{3\text{dB,el}}/R_s$	1.10	0.85	1.50	0.90	1.25	0.60

Table 3
Optimal optical and electrical receiver filter BWs for DQPSK

SMF	back-to-back		$R_d = 221\,\text{ps/nm}$		$\Delta\tau = 30\,\text{ps}$	
configuration	NRZ	RZ	NRZ	RZ	NRZ	RZ
$\Delta f_{3\text{dB,opt}}/R_s$	1.2	2.2	1.4	1.1	3.1	2.4
$f_{3\text{dB,el}}/R_s$	1.10	0.70	0.70	0.60	1.25	0.60

[1] in order to simplify the notation we will use the term 'tolerance', even though the system parameters are no longer constant.

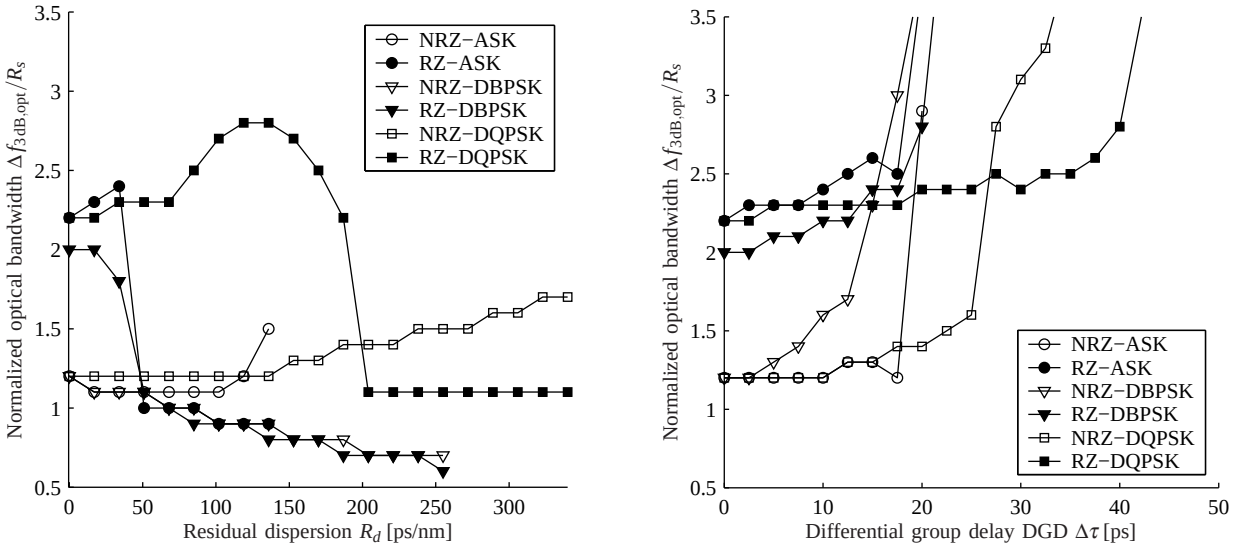

Fig. 8. Normalized optical BW $\Delta f_{3\mathrm{dB,opt}}/R_s$ vs. (a) residual dispersion and (b) differential group delay for various modulation formats

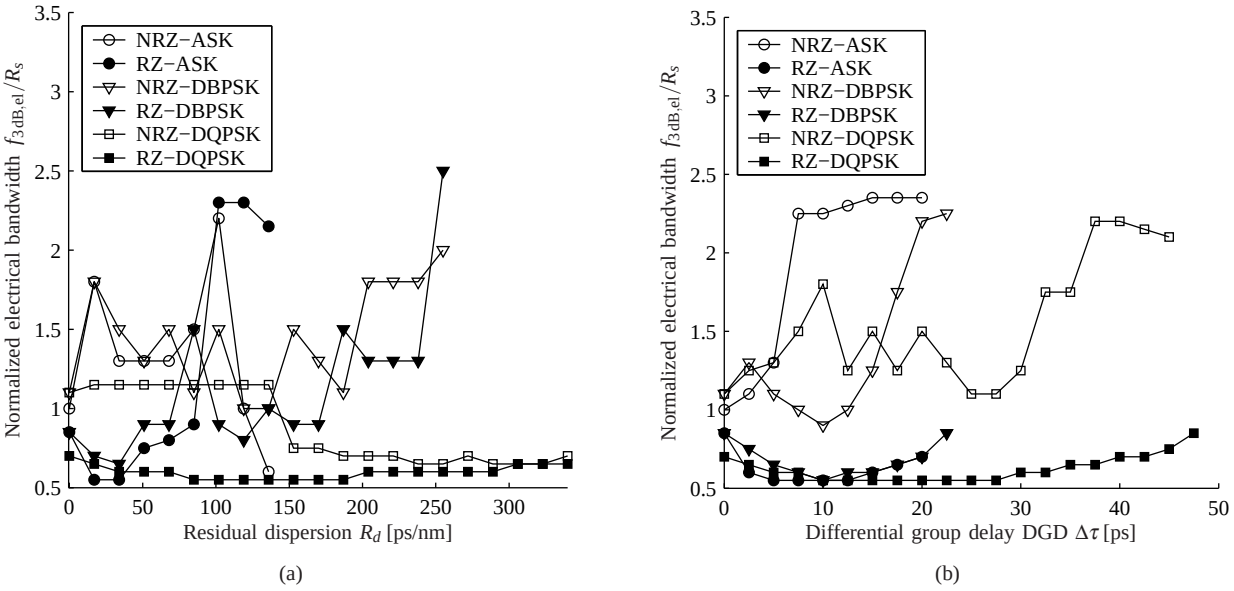

Fig. 9. Normalized electrical BW $f_{3\mathrm{dB,el}}/R_s$ vs. (a) residual dispersion and (b) differential group delay for various modulation formats

The results for the optimum BWs for DQPSK are not shown graphically due to the fact that the behaviour is qualitatively the same as for DBPSK. Nevertheless, **Table 3** gives an overview of the results for the bandwidth optimization for DQPSK again for the b2b case, the case where PMD is absent and $R_d = 221\,\mathrm{ps/nm}$, and the case where CD is absent and $\Delta\tau = 30\,\mathrm{ps}$.

Fig. 8 shows the optimal normalized optical BW $\Delta f_{3\mathrm{dB,opt}}/R_s$ vs. (a) residual dispersion R_d and (b) DGD $\Delta\tau$, respectively. In subfigure (a) the abscissa does only show positive values of R_d since the behaviour is symetrically as a good approximation. We can observe that the optical BW remains almost constant over the considered range of residual dispersion in case of NRZ impulse shaping. Opposed to that for RZ impulse shaping the optimal optical BW significantly decreases for RZ-ASK from $2.2 \cdot R_s$ for $R_d = 0$ to $0.9 \cdot R_s$ for $R_d = 136\,[\mathrm{ps/nm}]$, for RZ-DBPSK from $2.0 \cdot R_s$ for $R_d = 0$ to $0.6 \cdot R_s$ for $R_d = 255\,[\mathrm{ps/nm}]$, and for RZ-DQPSK from $2.2 \cdot R_s$ for $R_d = 0$ to $1.1 \cdot R_s$ for $R_d \geq 204\,[\mathrm{ps/nm}]$. Subfigure (b) shows that the dependence of the optical BW on PMD is vice versa: For both NRZ and RZ impulse shaping $\Delta f_{3\mathrm{dB,opt}}/R_s$ increases considerably for $\Delta\tau \geq T/2$, where $T = 25\,\mathrm{ps}$ for ASK and DBPSK and $T = 50\,\mathrm{ps}$ for DQPSK.

In **Fig. 9** the same is shown for the electrical BW $f_{3\mathrm{dB,el}}$. Again subfigures (a) and (b) show the dependence on the residual dispersion and on the DGD, respectively.

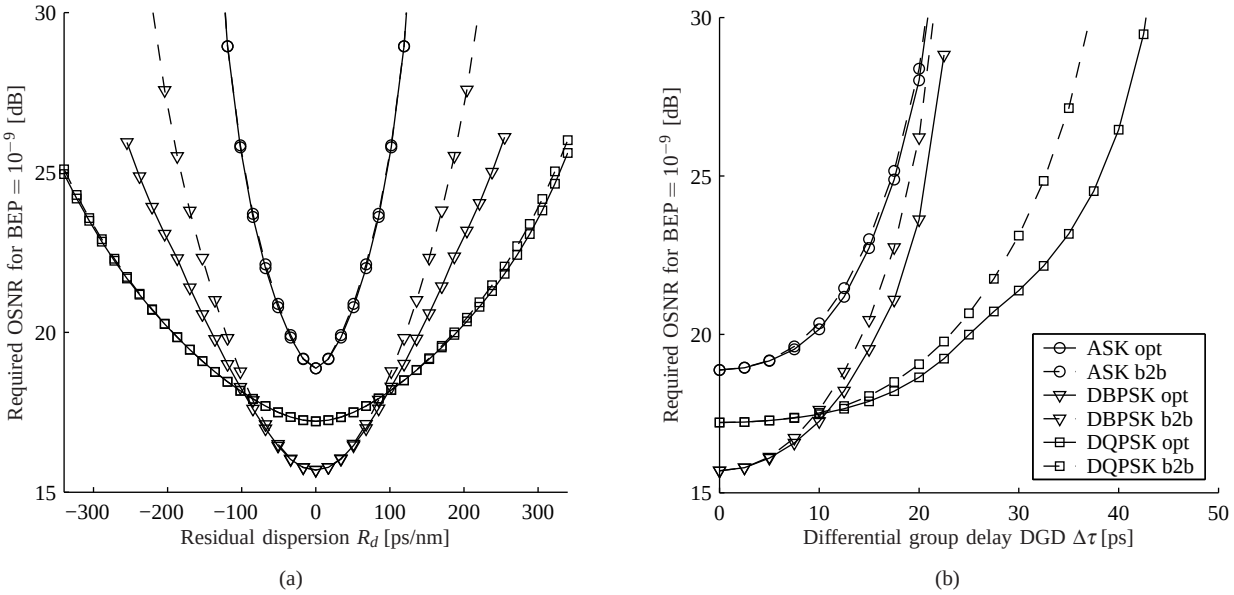

Fig. 10. Required OSNR for BEP $= 10^{-9}$ vs. (a) residual dispersion and (b) differential group delay for NRZ impulse shaping

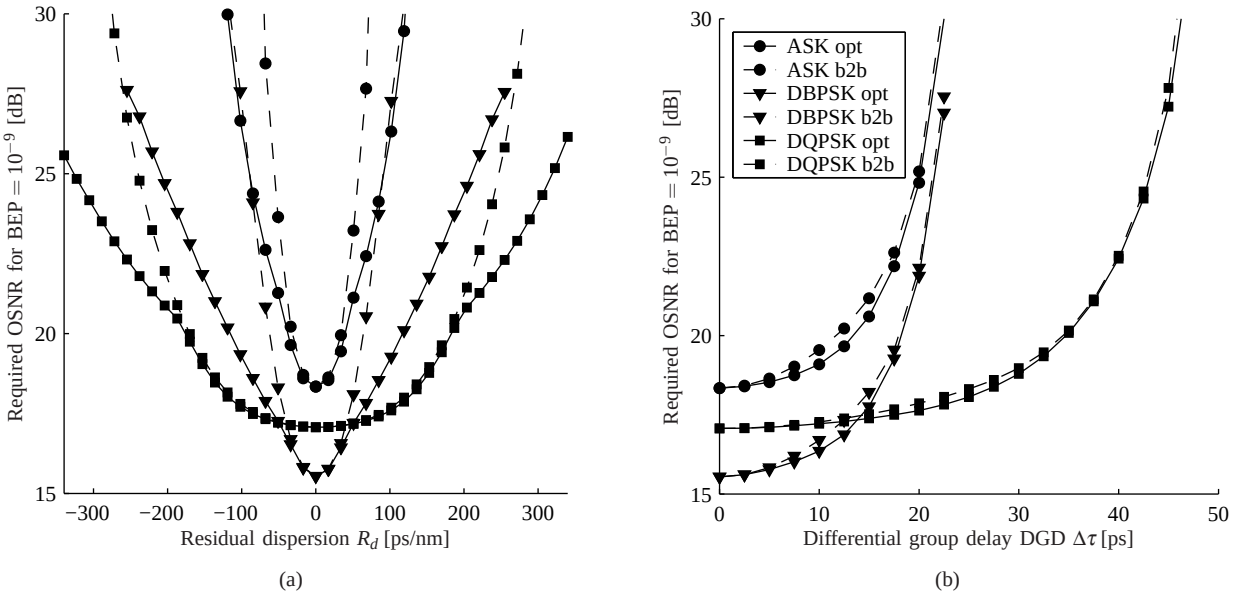

Fig. 11. Required OSNR for BEP $= 10^{-9}$ vs. (a) residual dispersion and (b) differential group delay for RZ impulse shaping

Obviously, a general tendency is no longer observable especially in case of CD. Only for DQPSK we can say that the electrical BW $f_{3\text{dB,el}}$ stays almost constant for RZ-DQPSK and decreases from about $1.1 \cdot R_s$ for $R_d = 0$ to about $0.7 \cdot R_s$ for $R_d \geq 187$ [ps/nm] for NRZ-DQPSK. For ASK and DBPSK $f_{3\text{dB,el}}/R_s$ shows a dithering performance when plotted vs. residual dispersion, which may be explained by recalling the fact that we observed a wide 0.3 dB penalty region with respect to the electrical BW in Figs. 6(b) and 7(b) and therefore a variation of the electrical BW does not have much effect on the required OSNR. The dependence of $f_{3\text{dB,el}}$ on DGD shown in Fig. 9(b) is again more clear: For RZ impulse shaping $f_{3\text{dB,el}}$ remains almost constant between $0.5 \ldots 0.9 \cdot R_s$, whereas for NRZ impulse shaping we can again observe that $f_{3\text{dB,el}}$ increases to values around $2 \ldots 2.5 \cdot R_s$ if $\Delta\tau$ becomes larger than $T/2$.

Finally we show CD and PMD tolerance of ASK, DBPSK and DQPSK for NRZ and RZ impulse shaping in **Fig. 10** and **Fig. 11**. Subfigures (a) and (b) present the required OSNR for $BEP = 10^{-9}$ vs. residual dispersion R_d and DGD $\Delta\tau$, respectively. The dashed curves correspond to the case where the optical and electrical BWs have only been optimized for b2b transmission and have then further been considered as constant. Opposed to that, the solid curves represent the case where we used optimized BWs for every marked point according to Figs. 8 and 9. As can be observed from

Table 4
Tolerable CD ΔR_d for OSNR penalty of 3 dB

ΔR_d [ps/nm]	ASK		DBPSK		DQPSK	
for 3 dB penalty	NRZ	RZ	NRZ	RZ	NRZ	RZ
back-to-back BW	129	81	201	107	397	361
optimized BW	132	106	223	169	402	363

Table 5
Tolerable DGD $\Delta\tau$ for OSNR penalty of 3 dB

$\Delta\tau$ [ps]	ASK		DBPSK		DQPSK	
for 3 dB penalty	NRZ	RZ	NRZ	RZ	NRZ	RZ
back-to-back BW	13.2	15.3	12.3	15.6	23.8	34.7
optimized BW	13.6	16.2	13.4	16.3	25.8	34.9

Fig. 10(a) the optimization of the BWs does not yield a significant improvement in CD tolerance for NRZ impulse shaping except for DBPSK where we can observe some improvement in a range where $|R_d| > 100$ ps/nm. However in this range the OSNR penalty with respect to the b2b case is already larger than about 3 dB. From Fig. 10(b) it becomes obvious that the PMD tolerance for NRZ impulse shaping may only be slightly improved for DBPSK and DQPSK whereas the improvement is negligible for ASK. The most significant improvement we can observe for the CD tolerance for RZ impulse shaping in Fig. 11(a). Especially for ASK and DBPSK the 3 dB penalty is increased by 30% for ASK and even 60% for DBPSK. For DQPSK the CD tolerance is increased as well, however, first in a range where $|R_d| > 200$ ps/nm and the penalty is larger than 3 dB. From Fig. 11(b) we can conclude that the PMD tolerance may not be significantly improved for any of the regarded modulation format if RZ impulse shaping is applied. As a summary the tolerable residual dispersion ΔR_d and the tolerable DGD $\Delta\tau$ for 3 dB OSNR penalties with respect to the b2b values are given in **Table 4** and **Table 5**, respectively.

5 Conclusion

We have shown how to extend the KLSE method to take account of not only CD but also PMD and we used this method to calculate the required OSNR for $\mathrm{BEP} = 10^{-9}$. We investigated the impact of optical and electrical RX filter BWs on CD and PMD tolerances for ASK, DBPSK and DQPSK. We observed that the effect of optimizing BWs with respect to the amount of CD or PMD is limited when NRZ impulse shaping is applied. However, for RZ impulse shaping the CD tolerance can be significantly improved especially for ASK and DBPSK. We observed as well that the optimal optical BW decreases with the amount of CD at least for RZ, whereas it increases with the amount of PMD. As these are opposed requirements, we must conclude that a general rule of thumb how to adjust the RX BWs can not be given. In fact a joint optimization taking into account both CD and PMD has to be done for every system application individually.

References

[1] R. A. Griffin and A. C. Carter, "Optical differential quadrature phase-shift key (oDQPSK) for high capacity optical transmission," in *Proc. Opt. Fiber Comm. Conf.*, Anaheim, CA, USA, Mar. 2002, pp. 367–368.

[2] M. Ohm and J. Speidel, "Quaternary optical ASK-DPSK and receivers with direct detection," *IEEE Photon. Technol. Lett.*, vol. 15, no. 1, pp. 159–161, Jan. 2003.

[3] S. Hayase, N. Kikuchi, K. Sekine, and S. Sasaki, "Proposal of 8-state per symbol (binary ASK and QPSK) 30-Gbit/s optical modulation/demodulation scheme," in *Proc. Eur. Conf. Opt. Comm.*, Rimini, Italy, Sept. 2003, paper Th2.6.4.

[4] M. Ohm, "Optical 8-DPSK and receiver with direct detection and multilevel electrical signals," in *Proc. IEEE/LEOS Workshop on Advanced Modulation Formats*, Los Angeles, CA, USA, July 2004, pp. 45–46.

[5] F. Buchali and H. Bülow, "Adaptive PMD compensation by electrical and optical techniques," *J. Lightw. Technol.*, vol. 22, no. 4, pp. 1116–1126, Apr. 2004.

[6] H. F. Haunstein, W. Sauer-Greff, A. Dittrich, K. Sticht, and R. Urbansky, "Principles for electronic equalization of polarization-mode dispersion," *J. Lightw. Technol.*, vol. 22, no. 4, pp. 1169–1182, Apr. 2004.

[7] J. Wang and J. M. Kahn, "Performance of electrical equalizers in optically amplified OOK and DPSK systems," *IEEE Photon. Technol. Lett.*, vol. 16, no. 5, pp. 1397–1399, May 2004.

[8] V. Curri, R. Gaudino, A. Napoli, and P. Poggiolini, "Electronic equalization for advanced modulation formats in dispersion-limited systems," *IEEE Photon. Technol. Lett.*, vol. 16, no. 11, pp. 2556–2558, Nov. 2004.

[9] E. Forestieri, "Evaluating the error probability in lightwave systems with chromatic dispersion, arbitrary pulse shape and pre- and postdetection filtering," *J. Lightw. Technol.*, vol. 18, no. 11, pp. 1493–1503, Nov. 2000.

[10] J. Wang and J. M. Kahn, "Impact of chromatic and polarization-mode dispersions on DPSK systems using interferometric demodulation and direct detection," *J. Lightw. Technol.*, vol. 22, no. 2, pp. 362–371, Feb. 2004.

[11] T. Freckmann and J. Speidel, "Viterbi-equalizer with analytically calculated branch metrics for optical DBPSK and ASK with dominating ASE noise," in *Proc. 6th ITG Conf. on Photonic Networks*, Leipzig, Germany, May 2005, pp. 169–175.

[12] S. R. Chinn, D. M. Boroson, and J. C. Livas, "Sensitivity of optically preamplified DPSK receivers with fabry-perot filters," *J. Lightw. Technol.*, vol. 14, no. 3, pp. 370–376, Mar. 1996.

[13] A. O. Lima, I. T. Lima, T. Adali, and C. R. Menyuk, "Comparison of power penalties due to first- and all-order PMD distortions," in *Proc. Eur. Conf. Opt. Comm.*, Copenhagen, Denmark, Sept. 2002, paper 7.1.2.

[14] T. Freckmann, "Bit error probability evaluation for optical transmission systems with direct detection," Diploma thesis, University of Stuttgart, Institute of Telecommunications, Stuttgart, Germany, Apr. 2004.

[15] P. J. Winzer, M. Pfennigbauer, M. M. Strasser, and W. R. Leeb, "Optimum filter bandwidths for optically preamplified nrz receivers," *J. Lightw. Technol.*, vol. 19, no. 9, pp. 1263–1273, Sept. 2001.

[16] H. F. Haunstein, R. Schlenk, A. Dittrich, W. Sauer-Greff, and R. Urbansky, "Optimized filtering for electronic equalizers in the presence of chromatic dispersion and PMD," in *Proc. Opt. Fiber Comm. Conf.*, Los Angeles, CA, USA, Feb. 2004, paper MF63.

[17] M. Ohm and J. Speidel, "Optimal receiver bandwidths, bit error probabilities and chromatic dispersion tolerance of 40 GBit/s optical 8-DPSK with NRZ and RZ impulse shaping," in *Proc. Opt. Fiber Comm. Conf.*, Anaheim, CA, USA, Mar. 2005, paper OFG5.